ISSN 1063-7745, Crystallography Reports, 2021, Vol. 66, No. 1, pp. 142–155. © Pleiades Publishing, Inc., 2021.
Russian Text © The Author(s), 2021, published in Kristallografiya, 2021, Vol. 66, No. 1, pp. 135–148.

CRYSTAL GROWTH

Crystallomorphological and Crystallochemical Indicators of Diamond Formation Conditions

Yu. N. Palyanov[a,b,*], A. F. Khokhryakov[a,b], and I. N. Kupriyanov[a]

[a] *Sobolev Institute of Geology and Mineralogy, Siberian Branch, Russian Academy of Sciences, Novosibirsk, 630090 Russia*
[b] *Novosibirsk State University, Novosibirsk, 630090 Russia*
**e-mail: palyanov@igm.nsc.ru*

Received July 2, 2020; revised August 6, 2020; accepted August 6, 2020

Abstract—An analytical review of the results of experimental studies of diamond crystallization and dissolution in systems with different compositions and mantle $P–T$ parameters is presented. It is shown that the diamond morphology and the set of defect-impurity centers depend to a great extent on the composition of crystallization medium. Specific crystallomorphological and crystallochemical features of diamond that are typical of certain conditions are revealed. The genetic informativeness of some diamond characteristics and possibility of their use as indicators of the composition of crystallization and dissolution media and oxygen fugacity in diamond-origin processes are substantiated based on the experimentally established regularities in the "conditions–properties" system.

DOI: 10.1134/S1063774521010119

CONTENTS

INTRODUCTION

An analysis of the data on the mineralogy of natural diamond shows that crystals from different deposits have fairly diverse characteristics (including morphology, composition of the mineral and fluid inclusions, and a set of defect-impurity centers), a fact suggesting a wide variety of their formation conditions in nature. Complex studies of diamonds from different regions of the world made it possible to determine the main diamond-containing paragenesises, the range of $P–T$ formation conditions, age, key characteristics of the defect-impurity composition of diamonds, and regularities of the isotopic carbon composition, as well as to form a concept about diamond origin [1–20]. Of prime importance are the data on the composition of microinclusions in diamonds, because specifically they give idea about the compositions of the diamond-forming media [12, 21–31]. The case in hand is primarily high-density fluids (containing carbonates, silicates, chlorides, water, and CO_2) and the fluids of the C–O–H–N system. Another important result is the discovery of inclusions in diamonds, which serve as indicators of redox conditions. A very broad range of variation in the compositions was established: from strongly reduced (iron, moissanite, iron carbides) [17, 32–36] to extremely oxidized (CO_2, carbonates) [33, 37, 38]. There is no doubt that the crystallomorphological and crystallochemical features of diamond are potential sources of information about its formation conditions. However, the genetic informativeness of these features has been substantiated to date in only some particular cases. The main method for establishing the crystallomorphological and crystallochemical indicator characteristics of diamond is the experimental simulation of the natural processes of its formation, dissolution, and thermobaric treatment in a maximally wide range of compositions and conditions. Despite the fact that experiments on diamond crystallization in the systems simulating natural diamond-forming media have been actively performed in recent years, the data on the real structure and properties of diamonds obtained in these systems are still limited.

In this review, we analyze the results of experimental studies on diamond crystallization and dissolution in systems of different compositions, aimed at revealing regularities of diamond crystallomorphological features, characteristic of specific growth and dissolution conditions. The regularities of changes in the defect-impurity structure of diamond have been considered in dependence of the composition of the medium and the crystallization conditions. The

Table 1. Forms of diamond growth in different media

Crystallization-medium composition	Diamond growth forms	References
Metal melts (Fe, Ni, Co, Mn)	{111}, {100}, {110}, {311}, {511}, {711}	[44–46]
Sulfide melts (FeS, $(Fe, Ni)_9S_8$)	{111}	[50, 51]
S–C system	{100}, {111}, {411}, {944}	[47–49]
$CaCO_3$ melt	{533}, {955}, {755}, {211}, {322}	[53, 54]
Carbonate–silicate (including kimberlite) melts	{111}	[60–65]
Ultrapotassium carbonate, carbonate–silicate, and carbonate–chloride melts	{111}, {100}	[55–59]
Fluid media of the C–O–H system	{111}	[71–74]
Water-containing silicate melts	{111}	[75, 76]
Water-containing carbonate and carbonate–silicate media	{111}	[57, 59, 77, 78]
Na_2CO_3–CO_2–C system	{111}, {100}, {*hkk*}, {*hhl*}	[84]
P–C system	{111}, {310}, {911}	[66–68]
Mg–C system	{100}	[69]
Mg–C + Si (≥2 wt %) system	{111}	[70]

potential of the revealed regularities and specific characteristics of diamond as crystallomorphological and crystallochemical indicators of the conditions of diamond formation in natural processes is estimated.

1. DIAMOND CRYSTAL MORPHOLOGY AS AN INDICATOR OF CRYSTALLIZATION CONDITIONS

The morphology of natural diamonds is extremely diverse and specific; this holds true for not only contrast (with respect to geodynamic formation conditions) kimberlite and metamorphogenic diamonds but also for different kimberlite pipes and different fractions from the same deposit. For example, micro- and macrodiamonds have significantly different morphologies [20, 39, 40]. The following two factors affecting the morphology of different natural diamonds are most often considered when reconstructing their formation conditions: temperature and degree of supersaturation of medium with carbon. A pronounced temperature dependence of the change in diamond morphology in the cube–cuboctahedron–octahedron series was established in the early studies on diamond synthesis in metal–carbon systems [41, 42] and confirmed repeatedly in later publications. A similar dependence was also suggested for natural diamonds [2]. The growth of morphologically different natural diamonds with different degrees of structural quality, depending on the degree of supersaturation of the crystallization-medium with carbon, was described in [43].

During the last decade, the diamond crystallization in various systems (including model natural diamond-forming media) has been thoroughly studied experimentally (Table 1). It is of interest to analyze these experimental data and reveal the main regularities of changes in the diamond morphology in dependence of the crystallization conditions.

In the metal–carbon systems (the best studied ones from the point of view of diamond synthesis), the main growth forms are cube and octahedron; the additional ones are the rhombododecahedron faces and faces of tetragontrioctahedra {311}, {511}, and {711} [44–46]. With an increase in temperature, the habit of diamond crystals gradually changes from cube to octahedron. In the case of diamond synthesis in the S–C system, cube faces are dominant, the {111} faces are less frequent, and the {411} and {944} tetragontrioctahedra are rare (Fig. 1a) [47–49]. A systematic change in the diamond morphology in the cube–octahedron series with an increase in temperature (however, less pronounced than in the metal–carbon systems) was also revealed in this system. In the melts of sulfides of pyrrhotite and pentlandite compositions, diamond is crystallized only as an octahedron [50, 51]. Taking into account the high P–T parameters of diamond synthesis in the sulfide–carbon systems, one would suggest that the octahedral form of diamond crystals can be controlled by temperature. However, when sulfur is added to the metal–carbon melt, even at relatively low temperatures (1400°C) the form of diamond growth from the metal–sulfide melt is an octahedron [52]. In the case of diamond crystallization from a carbon solution in the $CaCO_3$ melt, the main growth forms are the {533}, {955}, {755}, {211}, and {322} faces of a series of tetragontrioctahedra (Fig. 1b) [53, 54]. In the ultrapotassium carbonate, carbonate–silicate, and carbonate–chloride melts, the diamond habit is determined by the {111} and {100} faces (Fig. 1c) [55–59]. In the carbonate–silicate melts (including kimberlite ones), the stable diamond growth form is an octahedron (Fig. 1d) [60–65].

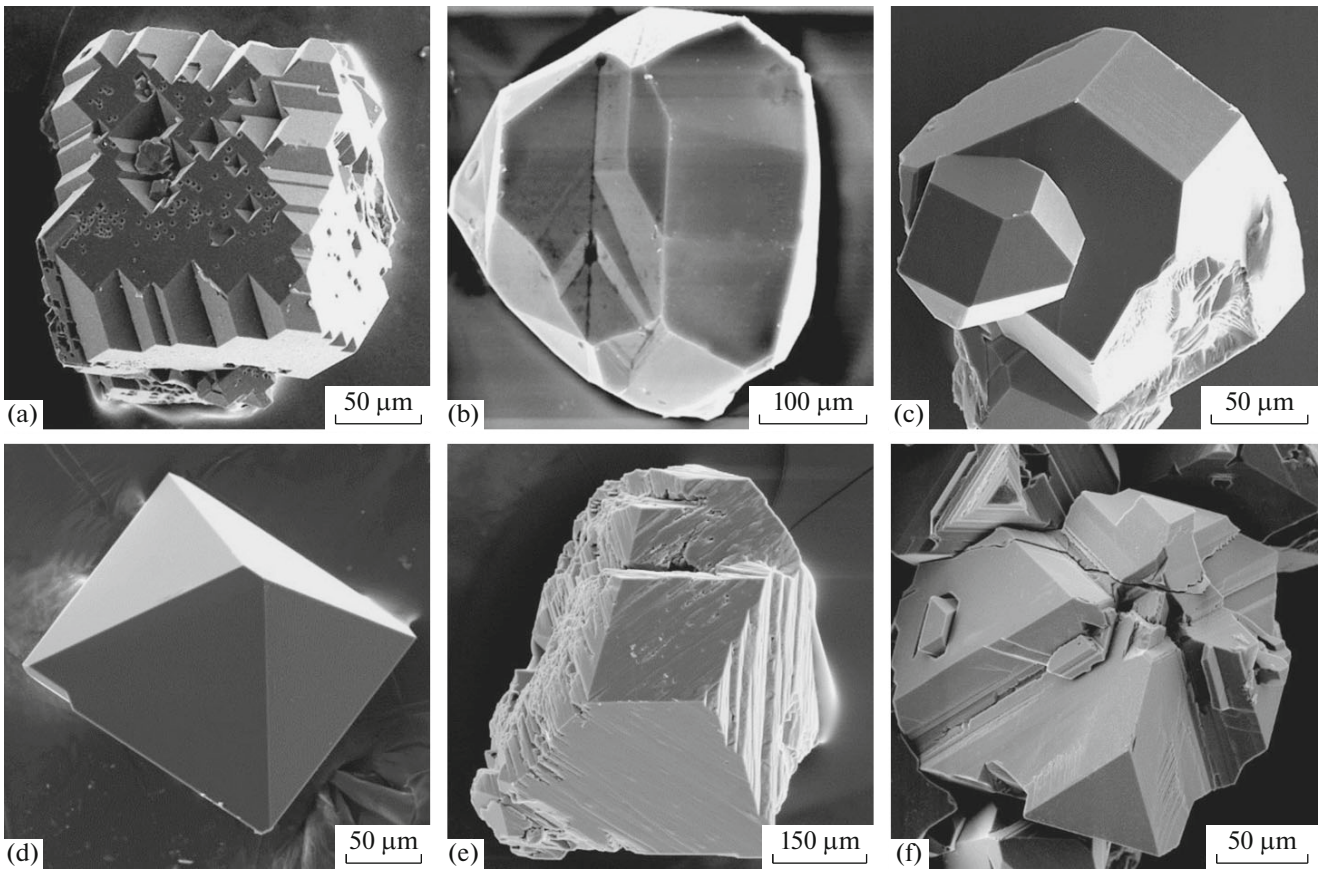

Fig. 1. Morphology of the diamond crystals obtained in different systems: (a) crystal with dominant {100} faces, S–C system; (b) twin of diamond crystals of complex combination form, $CaCO_3$–C system; (c) cuboctahedron, K_2CO_3–KCl–C system; (d) octahedron, Mg_2SiO_4–H_2O–C system; (e) rhombododecahedral diamond crystal, $Ni_{0.7}Fe_{0.3}$–H_2O–C system; and (f) antiskeletal diamond crystal, $Ni_{0.7}Fe_{0.3}$–H_2O–C system.

A morphology unusual for diamond was revealed in the phosphorus–carbon system: the growth forms were found to be the faces of octahedron, tetragon-trioctahedron {911}, and tetrahexahedron {310} [66–68]. A strong influence of impurities on the diamond morphology can be illustrated by an example of the Mg–C system, in which diamond is crystallized only in the form of cubes [69]. However, when adding even a small amount of silicon (Si ≥ 2 wt %), a flat-face octahedron becomes the only growth form [70]. Thus, the data on diamond crystallization in fluidless melts of different compositions show that the diamond morphology depends to a great extent on the crystallization-medium composition and a systematic dependence of the crystal habit on temperature manifests itself only in individual cases (metal and sulfur melts). The data on diamond crystallization in the fluid media of the C–O–H system indicate that only the octahedral growth form is stable under these conditions [71, 74]. Since most modern models of diamond origin suggest an active role of fluids [2, 7–9, 16], it is expedient to estimate the influence of fluids of the C–O–H system on the diamond morphology. According to the existing experimental data, octahedron is the stable growth form in water-containing silicate [59, 75, 76], carbonate–silicate [57, 59, 77, 78], carbonate [55–57], and carbonate–chloride systems [57], which model the composition of natural high-density diamond-forming fluids.

Under natural conditions, the only flat-face diamond form is also an octahedron. Natural diamonds form either regular octahedra or crystals with lamellar-step (differently pronounced) structures with combination forms, up to crystals with a rhombododecahedral habit. It was shown experimentally for the metal–carbon system with H_2O additives that these diamond crystals are formed due to the antiskeletal growth of {111} faces when impurities are adsorbed [79, 80]. The morphology of antiskeletal diamond polyhedra is determined by the habit of the initial crystals, the structure of the lateral surfaces of growth pyramids of the {111} faces, and their development symmetry (Figs. 1d, 1e) [79, 80].

Natural diamond crystals with a cubic habit do not create flat-face forms. They are characterized by a cellular structure of faces, as well as curvilinear zonality

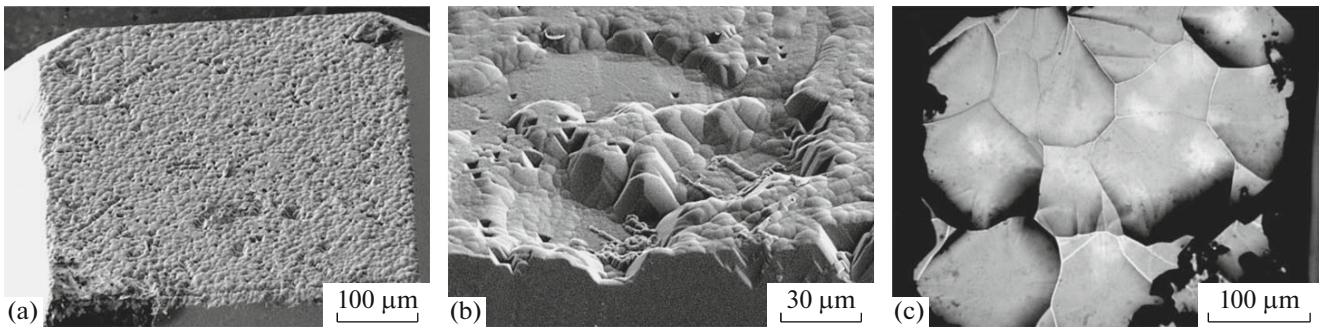

Fig. 2. Cellular structure of the {100} faces of diamond crystals synthesized in alkaline carbonate system: (a, b) $MgCO_3$–Na_2CO_3–SiO_2–CO_2–H_2O and (c) Na_2CO_3–CO_2.

or fibrous structure [81, 82]. The conditions providing cellular growth of the {100} faces of natural diamonds of the cubic habit and formation of a fibrous structure are still debated. There are scarce experimental data [83, 84] on their formation in the carbonate–silicate growth media enriched with a CO_2 fluid (Fig. 2). The cellular surface structure on the {100} diamond faces, formed by rounded hillocks, was found on the diamonds grown in an alkaline carbonate–silicate medium containing a water-carbon fluid [83]. In addition, diamond crystals with a structure of the growth sectors of {100} faces that is similar to the fibrillar structure of natural diamond cuboids were grown in the Na_2CO_3–CO_2–C system [84]. Experiments on growing diamond crystals in the Na_2CO_3–CO_2–C system on natural dodecahedroids (which can be considered as spheres) were carried out. As a result of the regeneration of dodecahedroids, it was established that cube and tetragon-trioctahedron faces, rounded octahedron faces, and rough {110} surfaces were formed in the initial growth stages. Rounded polyhedra of the octahedral habit with rounded surfaces; tetragontrioctahedron {*hkk*}, trigontrioctahedron {*hhl*}, and cube {100} faces; and specific vicinal relief were formed in the final stage [84].

An analysis of the aforementioned data shows that the diamond morphology is determined mainly by the crystallization-medium composition. By an example of diamond crystallization in the metal–carbon system with addition of nitrogen-containing compounds, systematic changes in the diamond morphology and structural quality were also revealed [85]. An increase in the nitrogen content in the crystallization medium leads to systematic changes in crystal faceting: {111} > {100}, {311}, {110} → {111} > {100}, {311} → {111} ≫ {100} (with the P–T parameters maintained constant). Simultaneously with changes in the crystal faceting, the structural quality of diamonds changes significantly according to the following scheme: single crystals → block crystals with microtwins → aggregates of block crystals and twins. With an increase in the nitrogen content in the crystallization medium, the density of dislocations and twin lamellae in diamonds increases significantly, an anomalous birefringence (caused by the internal stress) increases, and intense capture of inclusions occurs.

Many of studies aimed at interpreting the formation conditions of morphologically different natural diamonds are based on the concepts about the decisive role of crystallization-medium supersaturation with carbon [43]. Experimental implementation of diamond crystallization conditions at different controlled supersaturations with high P–T parameters is a fairly complex problem. The influence of supersaturation on the diamond growth and morphology was revealed using a metal–carbon system characterized by the maximum carbon solubility [86]. The use of different crystallization schemes and growth methods made it possible to implement diamond crystallization at different supersaturations with a change in the linear diamond-growth rate in a very wide range: from ~10^{-1} μm/h to more than ~10^4 μm/h. It was established that, at weak supersaturations and low growth rates, the diamond morphology is determined by the {110}, {111}, {100}, and {*hkk*} faces. With an increase in the supersaturation and growth rate, the crystal faceting is determined by only the cube and octahedron faces, the ratio of which in this system depends on temperature. The sequence of a change in the external appearance of crystals, related to the increase in supersaturation and growth rate, was found to be as follows: needle-like crystals → bulk flat-face crystals, skeletal crystals → dendrites → aggregative crystals → polycrystalline aggregates.

Based on the analysis of the data on the morphology of diamonds synthesized in systems with radically different compositions in a wide range of crystallization conditions one can formulate the following main regularities:

(i) the main factor affecting the diamond growth forms and structural quality is the crystallization-medium composition;

(ii) the dominant diamond-growth form in the systems modeling most of natural diamond-forming media is octahedron;

(iii) the variety of the morphology of diamond of octahedral growth form is due to the impurity adsorption influence, which leads to the formation of antiskeletal crystals;

(iv) crystals having cube faces with cellular or vicinal surfaces and fibrillar structure of the growth sectors of {100} faces were experimentally obtained only in specific alkaline carbonate and carbonate-silicate systems containing a CO_2 fluid. Crystals of this type can be indicators of the alkaline carbonate-containing media with a dominant carbon fluid.

2. INDICATOR ROLE OF DEFECT-IMPURITY CENTERS IN DIAMOND

One of potential sources of information about the genetic history of diamond is the specificity of its defect-impurity structure. It is well known that natural diamonds are characterized by an unusually wide spectrum of defect-impurity centers, which is related to the wide range of variation in their formation conditions and the post-growth history (including mantle annealing and mechanical effects causing plastic deformation). To date, a fairly large number of types of impurities that can be incorporated isomorphically into the diamond lattice have been found. Generally, many defect-impurity centers can be formed in the diamond structure even on the basis of a single chemical element. For example, nitrogen, being the most widespread impurity in diamond, can form up to several tens of different centers. The main structural impurities in natural diamonds are nitrogen, hydrogen, and boron. Defects caused by nickel and silicon impurities have also been identified. The results of the recent studies in this field indicate that defects related to oxygen [87] and titanium [88] impurities can also be present in natural diamonds. Along with the aforementioned impurities, synthetic diamonds formed in different growth systems were found to contain impurity centers based on phosphorus, cobalt, germanium, tin, and (presumably) iron [89] and oxygen [84]. Undoubtedly, the information about the specific features of the internal structure of natural diamonds and their defect-impurity composition constitutes an immense data array, which is of fundamental importance for reconstructing the diamond formation conditions. However, adequate interpretation of these data calls for the knowledge of reliably established relationships in the "conditions–properties" system. In this context, the experimental studies of the crystallization-conditions influence on the formation of defect-impurity centers in diamond are of great importance. Note that these studies are very important for not only Earth sciences but also for the interdisciplinary studies aimed at producing diamonds with specific properties for high-tech applications.

As was noted above, nitrogen is the main structural impurity in both natural and synthetic diamonds. The form and concentration of nitrogen centers determine to a great extent many physical properties of diamond. The main nitrogen centers are single substitutional nitrogen atoms (*C* centers), atomic pairs (*A* centers), and more complex aggregates (*B*1 and *B*2 centers). Most of synthetic diamonds obtained in conventional metal–carbon systems contain nitrogen impurity mainly in the form of *C* centers (Ib type). In contrast, the overwhelming majority of natural diamonds (98–99%) contain nitrogen impurity in the aggregated form (Ia type). According to the generally accepted annealing model of the formation of complex nitrogen centers in diamond, the initial form of incorporation of impurity nitrogen into the diamond lattice is *C* centers. Different defect aggregates, containing two (*A* centers); three (*N*3 centers); four (*B*1 centers); and, possibly, more (*B*2 centers, voidites) nitrogen atoms, are formed from these centers due to the thermally activated diffusion during mantle annealing [90]. The process of impurity-nitrogen aggregation can be separated qualitatively into two stages. In the first stage, *A* centers arise, from which more complex defects (mainly *B*1 centers) are formed in the second stage [91–96]. The main experimental studies of the processes of formation of *A*, *B*1, *B*2, and *N*3 defects (which are the main indicators of the influence of high-temperature annealing) were performed by the Evans' research team (University of Reading, UK) [91–94]. Modern popular methods for estimating the time (geochronometer) and/or thermal (geothermometer) conditions of existing natural diamonds in the mantle are based on the established regularities of transformation of impurity nitrogen centers in diamond upon high-temperature annealing.

Significant differences in diamonds are determined by not only the form but also the concentration of defect-impurity centers (primarily, nitrogen). Natural diamonds are characterized by an extremely wide range of impurity-nitrogen concentrations. Both nitrogen-free crystals (≤~1 ppm, type IIa) and diamonds with nitrogen concentrations of about 2000–3000 ppm are known [97, 98]. The record values of the impurity-nitrogen concentration in natural diamonds (up to 5000 ppm) were found for the Kokchetav diamonds [99, 100]. Synthetic diamonds grown in metal–carbon systems contain generally nitrogen impurity in amounts of about 100–300 ppm [101]. Here, the source of this element is the nitrogen impurity in the initial reagents and the atmospheric nitrogen, which is present in pores of materials and high-pressure cell units. Crystals with maximum nitrogen concentrations in the range of 1000–2000 ppm were obtained in metal–carbon systems with addition of nitrogen-containing compounds (NaN_3, Fe_3N, $CaCN_2$, etc.) [85, 102, 103]. It was established in [85] that, with an increase in the nitrogen concentration (C_N) in the growth system from 0.005 to 0.6 at %, growth of single-crystal diamond passes to the formation of an aggregate of block twinned crystals and then to crystallization of metastable graphite. In the stage of sin-

gle-crystal growth, an increase in the C_N value causes a rise in the nitrogen concentration in diamond from 200 to 1080 ppm. A further increase in C_N leads to the formation of an aggregate of block crystals with a nitrogen concentration of about 120–300 ppm.

The results of the studies devoted to the synthesis and characterization diamond in nonmetallic systems (including model systems with compositions similar to those of natural mantle diamond-forming media) are of particular interest. A specific feature of nonmetallic systems is that the growth of relatively large crystals (with sizes necessary for spectroscopic studies) in these systems calls for a much higher temperature and/or duration of growth experiments than in the case of metal–carbon systems. In addition, diamond crystallization in some systems may occur only at relatively high temperatures (~1700–1800°C). Therefore, when interpreting the results, one must take into account the fact that the defect-impurity structure of diamond crystals was formed in this case under the joint effect of the growth and annealing processes.

Below, we will consider the results of studying the defect-impurity composition of the diamonds grown in carbonate, carbonate–silicate, chloride, and sulfide melts and in fluid and fluid-containing systems [50, 83, 104–106]. It should be noted that all experiments were carried out without adding nitrogen-containing compounds into the crystallization medium. It was found [105] for the diamonds grown in the $CaCO_3$–C system (7 GPa, 1750°C) that the impurity-nitrogen concentration in the crystals was varied in the range from 600 to 1500 ppm, which significantly exceeds the values characteristic of diamonds from metal–carbon systems (Fig. 3). The dominant form of impurity nitrogen is nitrogen pairs occupying neighboring substitution sites (*A* centers), which is obviously due to the relatively high crystallization temperature. Along with the impurity nitrogen centers, defects caused by hydrogen impurity (3107 cm^{-1} center) were found in the crystals studied. Hydrogen is known to be the second (in abundance) impurity in diamond, and the 3107 cm^{-1} center is characteristic of most of natural diamonds of the Ia type.

The diamonds crystallized from the carbon solution in melts of carbonates, chlorides, and sulfides at relatively high temperatures (≥1700°C) are characterized mainly by the presence of *A* centers and hydrogen-containing defects. High nitrogen concentration in diamonds (from 500 to 1500 ppm) was observed in all cases. With a decrease in the diamond-crystallization temperature to 1400–1600°C in alkaline carbonate–fluid and carbonate–silicate systems, formation of *A* and *C* centers was observed, and a tendency to a significant increase in the nitrogen-impurity content in diamonds with a change in the crystallization-medium composition from carbonate to carbonate–silicate was revealed. Addition of H_2O to carbonate and carbonate–silicate systems decreased significantly the nitrogen concentration in diamond and led to the crystallization of diamonds with a low nitrogen content (<100 ppm) in the H_2O–C system (Fig. 3). Note that addition of H_2O to the metal–carbon systems also decreased the nitrogen concentration in diamonds and gave rise to IR absorption bands due to hydrocarbon inclusions [79, 80].

Thus, the experimental results showed that the nonmetallic diamond-forming media provide more favorable conditions for the nitrogen-impurity incorporation into the diamond structure (~1000 ppm) as compared with metal–carbon systems (~150 ppm). In addition, the incorporation of the hydrogen impurity into diamond with the formation of the 3107 cm^{-1} centers was established for a large variety of nonmetallic solvents (including carbonates, silicates, chlorides, and sulfides).

The structural defects related to silicon impurity are of great interest in view of their possible indicator properties. To date, it has been reliably established that the optically active center with a zero-phonon line (ZPL) at 737 nm is related to the silicon impurity, and its structure corresponds to a single Si atom occupying a double semivacancy (Si*V*) site. This center was identified for the first time in diamonds implanted with silicon ions [107]. Afterwards, it was shown in numerous studies that Si*V* centers are characteristic of the overwhelming majority of diamond films grown by chemical vapor deposition (CVD) [108, 109]. It is believed that the silicon source in this case is silicon substrates and/or quartz windows and other silicon-containing units of reaction chambers, which are subjected to plasma etching during diamond synthesis. The possibility of doping diamond with silicon impurity during growth in metal–carbon systems at high *P*–*T* parameters was demonstrated in [110]: it was found that diamond crystals containing Si*V* centers can be obtained in the Fe–Ni–C system by adding a nitrogen getter (1–2% Ti, Zr) at a relatively high concentration of Si additive (~10 wt %). It was shown recently that magnesium-based systems are highly efficient for doping diamond with silicon [69, 70]. It was revealed that the diamond crystals synthesized in the Mg–C system are characterized by intense photoluminescence due to Si*V* centers. The maximum concentration of Si*V* centers in the synthesized diamonds was estimated to be about 150–200 ppb, which is close to typical concentrations of Si*V* centers in silicon-doped CVD diamonds [111, 112]. It should be noted that the main source of silicon in the experiments on synthesizing diamond in the Mg–C system was the Si impurity in the initial reagents with a total concentration of about 0.01–0.02 wt %. Apparently, the extremely high efficiency of diamond doping with silicon and formation of Si*V* centers in magnesium-based systems is primarily related to their ultra-reducing conditions at an oxygen fugacity (fO_2) lower than that of iron–wustite (IW) buffer. This circumstance may explain the fact

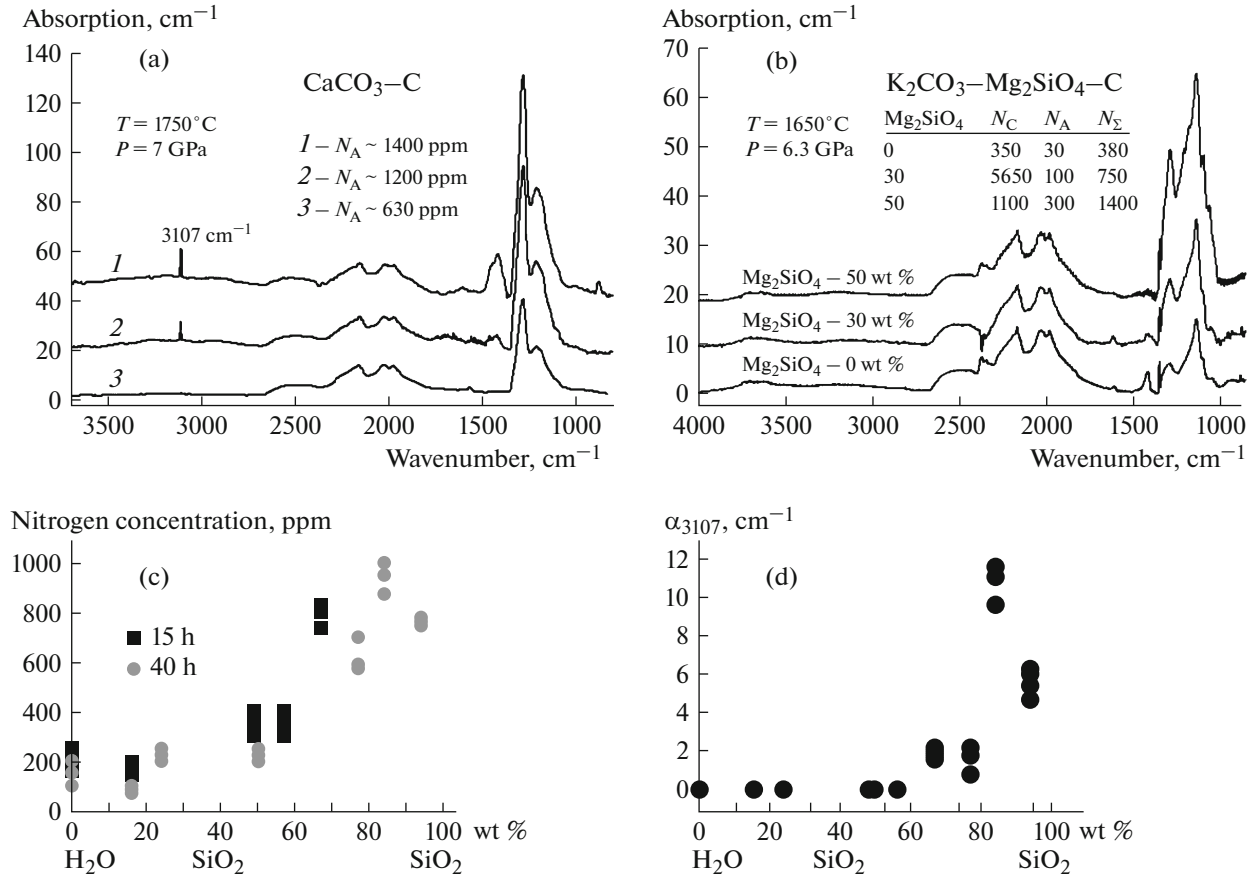

Fig. 3. IR absorption spectra of the diamonds synthesized in the (a) $CaCO_3$–C and (b) K_2CO_3–Mg_2CO_3–C systems [105]. The concentrations of nitrogen in the form of *A* centers (N_A) and *C* centers (N_C) and the total nitrogen content (N_Σ) are given in atomic parts per million (ppm). The IR spectra are shifted along the vertical axis for clarity. (c, d) Dependences of the (c) nitrogen impurity concentration and (d) absorption intensity of the peak at 3107 cm^{-1} on the SiO_2 content in the SiO_2–H_2O–C system [106].

that, according to the data in the literature, Si*V* centers are rare in natural diamonds. To date, there are only several studies reporting the presence of Si*V* centers in the photoluminescence spectra of few natural mantle diamonds [113, 114] and nanodiamonds from meteorites [115].

Some interesting results were obtained when studying the diamonds synthesized in the Na_2CO_3–CO_2–C system, which corresponds to the oxidative conditions with an oxygen fugacity in the range between the "graphite(diamond)–CO" (CCO) oxygen buffer and a value smaller than that for this buffer by 0.5 logarithmic units (CCO–0.5) [84]. The diamonds obtained at relatively low temperatures (1300–1400ºC) were found to have unusual IR absorption spectra in the defect-induced one-phonon region (Fig. 4). A band peaking at about 1065 cm^{-1}, which was presumably associated with oxygen-containing defects, dominates in the spectra. An electron spin resonance analysis of these crystals revealed some new centers, which can also be assigned to defects whose structure contains oxygen atoms [116, 117]. In natural diamonds, defects due to oxygen impurity have not been unambiguously identified yet. Note that the revealed band at 1065 cm^{-1} lies in the frequency range, characteristic of silicate inclusions in diamond; this circumstance may hinder its identification to a certain extent. Currently, the problem of oxygen defect-impurity centers in diamond is being actively studied [118–120].

Thus, one can conclude the following:

(i) high nitrogen concentration (≥1000 ppm) and presence of hydrogen-containing centers (3107 cm^{-1}) are indicators of nonmetallic diamond-forming media;

(ii) low nitrogen concentration (50–200 ppm) and occurrence of hydrocarbon inclusions are characteristic of diamonds grown in metal–carbon systems (+H_2O);

(iii) Si*V* centers in diamonds are indicators of reducing conditions ($fO_2 \leq$ IW) and nitrogen-free media;

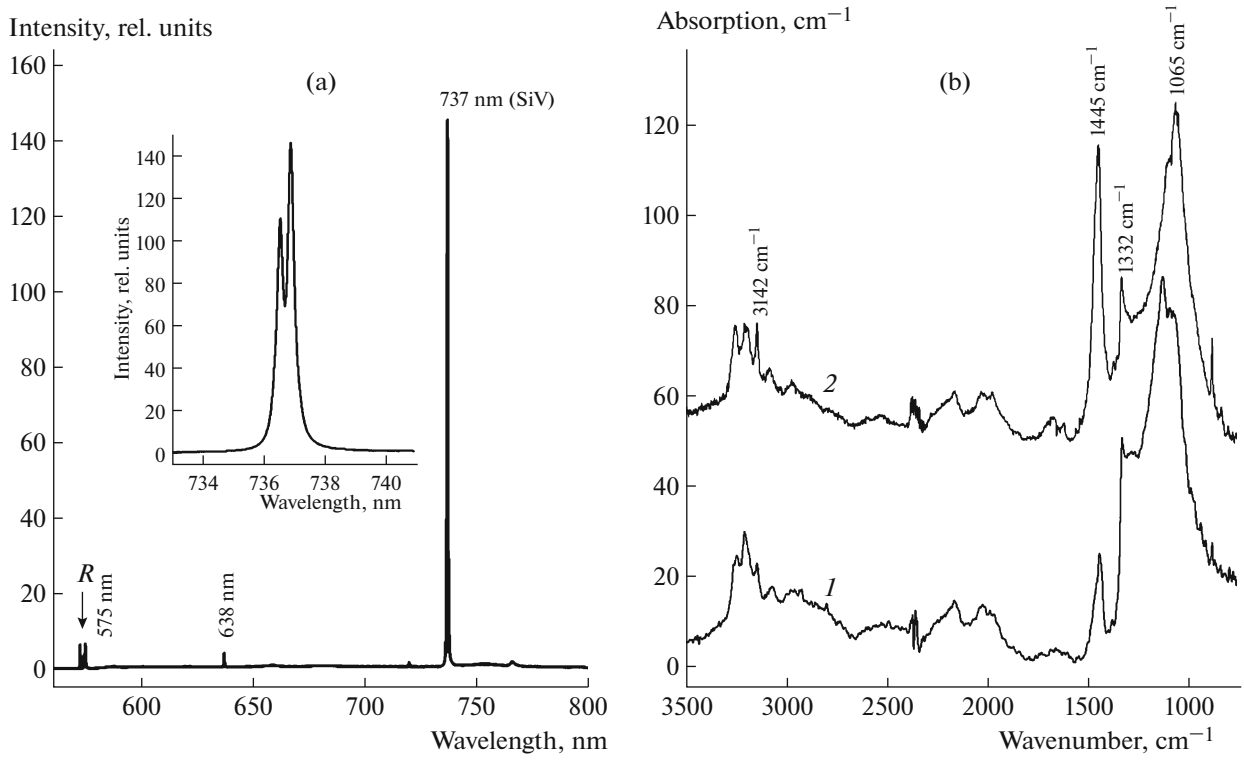

Fig. 4. (a) Typical photoluminescence spectrum of diamond crystals synthesized in the Mg–C system [69, 70]. *R* is the Raman scattering peak for diamond. (b) Typical IR absorption spectra of diamonds synthesized in the Na_2CO_3–CO_2–C system at temperatures in the range of 1300–1400°C [84]. The IR spectra are shifted along the vertical axis for clarity.

(iv) oxygen-containing centers (1065 cm^{-1}) are indicators of oxidative conditions (at fO_2 values ranging between CCO and CCO–0.5 logarithmic units).

3. DIAMOND CRYSTAL MORPHOLOGY AS AN INDICATOR OF DISSOLUTION CONDITIONS

A characteristic feature of natural diamond crystals is their rounded shape. Currently, there is hardly any doubt that the rounded shape of natural diamond is the result of dissolution of flat-face diamond crystals in kimberlite magma in the stage of its rise from the mantle to the Earth's surface. A detailed crystallographic description of these diamonds was provided by Fersman [121], Shafranovskii [122], Kukharenko [123], and Orlov [124, 125]. From a strictly crystallographic point of view, judging by the presence of edges and vertices, these diamonds are rounded tetrahexahedra or tetrahexahedroids [126, 127]. The variety of tetrahexahedroids manifests itself in different surface curvatures and angles between neighboring rounded surfaces. The curvature of tetrahexahedroids is estimated quantitatively according to the technique developed by Shafranovskii [122], who proposed to measure the angles of light triangles *ABC*, obtained on a photogoniometer from rounded surfaces. Undoubtedly, the specific features of the rounded shape of natural-diamond crystals and details of their surface microrelief reflect the diamond-dissolution conditions and the specificity of real crystal structure, as was confirmed experimentally by simulating the processes of natural dissolution of diamond.

During the last three decades, a significant amount of experimental data on simulating the natural dissolution of diamond have been accumulated. It was proven unambiguously that diamond tetrahexahedroids are formed during dissolution of flat-face diamond crystals in water-containing carbonate, silicate, and carbonate–silicate melts or fluids in wide ranges of temperatures and pressures (Figs. 5a, 5b) [128–137]. Complete absence of water in a system leads to the formation of either rounded specific crystals in carbonate melts (Figs. 5c, 5d) [137] or trigon-trioctahedroids in silicate melts [128]. These dissolution forms are extremely rare in natural diamonds. It was found experimentally that dissolution of natural diamond occurred in a wide oxygen fugacity range: from the reducing conditions corresponding to the IW buffer [138] to the oxidative conditions close to the hematite–magnetite buffer [139]. This range corresponds to the existing estimates of possible fugacity of kimberlites [140]. In more reducing conditions, at the fO_2 value close to that of Ti–TiO_2 buffer, trigon-trioctahedral forms occur (Fig. 5e) [131]. The diamond dissolution in the carbonatite melt in the presence of Fe^{3+}

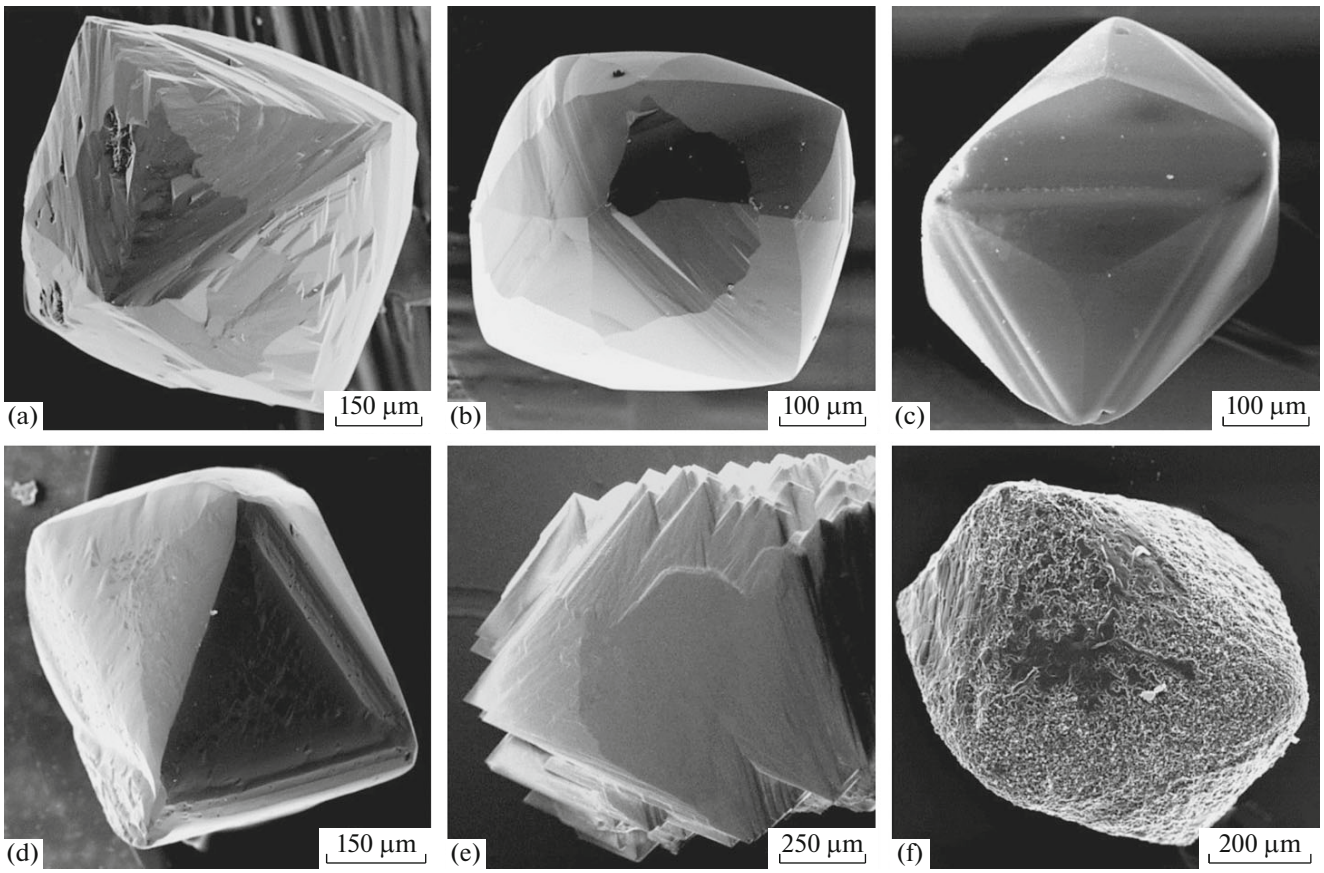

Fig. 5. Experimentally found dissolution forms of octahedral crystals of natural diamond in the following media: (a, b) water-containing carbonate and carbonate–silicate melts, (c) $CaCO_3$ melt, (d) carbonate melts + CO_2, (e) dissolution in fluid at an fO_2 value close to that for the Ti–TiO_2 buffer, and (f) carbonatite melt + Fe_2O_3.

induces the formation of corrosion sculptures [139], characteristic of the late stages of natural-diamond resorption (Fig. 5f).

It was shown experimentally that the curvature of rounded surfaces of tetrahexahedroids is related to the habit of the initial flat-face crystals and serves an indicator of the degree of their dissolution (preservation degree) [130, 133]. The evolution of dissolution forms was investigated for the three main habit types of natural diamond crystals: octahedron, rhombohedron, and cube (Fig. 6). It was established that diamond crystals pass through three evolution stages during dissolution. In the first stage, transition flat-face/curved-face forms occur, and relict faces of growth forms are retained on the crystals. In the second stage, tetrahexahedroids with rounded surfaces of various curvatures (depending on the habit of the initial diamond crystals) are formed. Based on the exterior similarity with flat-face crystals, they were referred to as octahedroids, dodecahedroids, and tetrahexahedroids (or cuboids), respectively, in the literature on natural diamonds [124]. In the final dissolution stage, tetrahexahedroids with constant curvatures $AB = 36°07'$, $CD = 13°15'$, and $DD' = 13°15'$ are formed. In this stage, crystals are dissolved without any significant changes in morphology, a fact indicating that they achieved a stationary diamond dissolution form (Fig. 6). In the literature on natural diamonds, this type of tetrahexahedroids is referred to as "Ural-type dodecahedroid" or "Brazil-type dodecahedroid" [123, 124]. As follows from Fig. 6, the transition from the first to the second stage and the formation of stationary dissolution form for crystals with different initial habits occur at different degrees of dissolution. This difference is related to the degree of deviation of the initial crystal form from the stationary diamond-dissolution form in the system under study. The revealed dependence of the morphology of diamond crystals on the loss of their initial mass (degree of dissolution) [130, 133] is of interest for practical problems of estimating the diamond-bearing potential of bedrock deposits.

Natural rounded diamonds also exhibit a large variety of surface sculptures. Generally, the surfaces of rounded diamonds contain various microrelief elements (including trigonal or hexagonal pits, ditrigonal and shield-like layers, drop-like hillocks, striation of various intensity, and other textures) [123, 125, 127, 141, 142]. Some crystals have macroscopically smooth

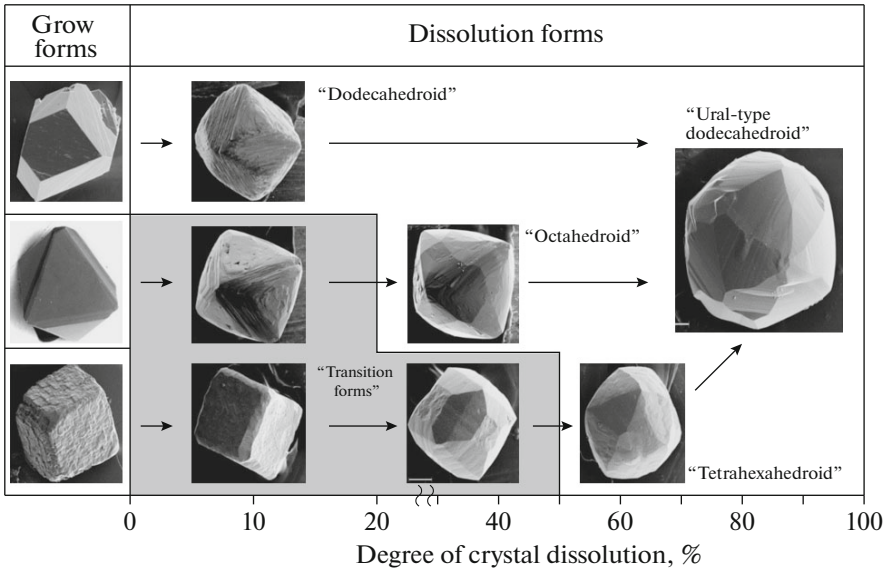

Fig. 6. Schematic of the crystallomorphological evolution of diamond crystals during dissolution in water-containing carbonate and silicate melts (according to the data of [130, 133]).

glossy surfaces. The reasons for the variety of sculptures on rounded natural diamonds are still insufficiently understood. For example, it was shown in [143] that the significant changes in the surface relief of natural diamonds may be related to the difference in the catalytic activity of ions involved in the natural-resorption process. It was shown that sculptures on the surfaces of natural diamond may be indicators of both the dissolution conditions and specific features of the internal structure of diamond crystals.

One of widespread relief elements of the flat- and curved-face forms of natural diamond are ditrigonal and shield-like layers on the relict {111} faces. It was unambiguously established that these layers (as well as the tetrahexahedroid crystal form on the whole) are a reliable indicator of diamond dissolution in the presence of water. For example, the presence of as little as 0.38 wt % water in a lamproite melt leads to diamond dissolution by ditrigonal layers along the {111} faces [129]. Another widespread relief element on {111} faces are triangular pits, oriented oppositely with respect to the octahedral-face contour. In the literature on natural diamonds they were referred to as "negative trigons" [144]. It was established that triangular etching pits on the {111} faces are located at the dislocation outcrops [145]. Sometimes hexagonal etching pits and positively oriented triangular pits are observed on natural diamond crystals. The experiments performed in gas media at high pressure showed that the trigon orientation is controlled by temperature and oxygen fugacity [146]. It should be noted that positive trigons become stable at a low temperature and under more oxidative conditions. However, an experimental study of the diamond dissolution in model fluid-containing carbonate–silicate melts revealed that the orientation of trigons is determined by the CO_2 content in the composition of volatile components of the dissolution medium and is independent of temperature and the fO_2 value [131, 134, 138]. The trigon orientation changes with a change in the $CO_2/(CO_2 + H_2O)$ ratio from 0.87 (formation of positive trigons) to 0.81 (formation of negative trigons) [134].

As was noted above, rounded surfaces of tetrahexahedroids of natural diamond are characterized by a large variety of microrelief features. A widespread element of the relief of natural diamond tetrahexahedroids is drop-like hillocks. Depending on the size, shape, and elongation of hillocks, their clusters form shagreen, block, or serrate types of microrelief on rounded surfaces. It was established experimentally that drop-like hillocks are characteristic microrelief forms of dissolution surfaces of mosaic diamonds, which are related to heavily stressed regions in crystals [135]. Thus, drop-like hillocks reflect primarily the specific features of the real structure of diamond crystals. Cutting hatching on tetrahexahedroids, which is related to the outcrops of plastic deformation bands in diamond onto the crystal surface, is also an indicator of the internal structure of diamond crystals [127]. The sectorial and zonal structures of diamond crystals also manifest themselves on rounded dissolution surfaces as specific positive and negative relief forms [147].

It was also experimentally found that the relief of rounded surfaces of natural-diamond tetrahexahedroids can also be an indicator of the redox conditions of natural-diamond dissolution in a kimberlite melt. The experiments on dissolving diamond in model

compositions of primary kimberlite magmas, which were in equilibrium with lithospheric peridotite, demonstrated that tetrahexahedroids have significantly different surfaces in dependence of the oxygen fugacity [139, 148]. Under moderately oxidative conditions, at the fO_2 values corresponding to Re–ReO_2 buffer, the surfaces are covered with a thin regular striation. At higher fO_2 values (corresponding to the magnetite–hematite buffer), the tetrahexahedroid surfaces are more roughly sculptured; they are formed due to the alternation of relatively smooth rounded surfaces of relief portions with irregular steps and very elongated hillocks. Both structural types of rounded surfaces are characteristic of natural rounded diamonds and can be indicators of oxygen fugacity in kimberlite magma.

Having summarized the review of experimental studies aimed at simulating the natural dissolution of diamond, one can draw the following main conclusions:

(i) the dissolution forms of a majority of natural diamonds (octahedroids, dodecahedroids) are indicators of partition of water-containing silicate and carbonate–silicate media in dissolution processes;

(ii) dissolution of natural diamond occurs in a wide range of oxygen fugacities: from the reducing conditions corresponding to the IW buffer to the oxidative conditions corresponding to the hematite–magnetite buffer;

(iii) the surface curvature of rounded natural diamonds is an indicator of the degree of their dissolution and can be used to estimate the diamond integrity and efficiency of ore bodies;

(iv) specific features of the microrelief of rounded surfaces of natural diamond reflect the dissolution conditions and specificity of the real crystal structure.

CONCLUSIONS

The analysis of the experimental results showed that some specific crystallomorphological and crystallochemical characteristics of diamonds are typical of certain diamond crystallization and dissolution conditions. The experimentally established regularities in the "conditions–properties" system make it possible to substantiate (with different probabilities) some diamond characteristics as indicators of the composition of crystallization and dissolution media and oxygen fugacity in the processes of diamond genesis. It is quite possible that there may be exceptions for some qualitative regularities. The main conclusions formulated in the end of each section, are based on the existing experimental data. We believe them to be useful for researchers in the fields of diamond mineralogy and interpretation of extremely complex questions of natural-diamond formation. Systematic and purposeful studies in experimental diamond mineralogy are undoubtedly urgent. In future, they will make it possible to solve a wider range of inverse problems: reconstruction of the formation conditions of various natural diamonds on the basis of their indicator properties.

FUNDING

The part of the study presented in Sections 1 and 2 was supported by the Russian Science Foundation (grant no. 19-17-00075), and the part presented in Section 3 was supported by the state assignment for the Sobolev Institute of Geology and Mineralogy of the Siberian Branch of the Russian Academy of Sciences.

REFERENCES

1. N. V. Sobolev, *Deep-Seated Inclusions in Kimberlites and the Problem on the Upper Mantle Composition* (Nauka, Novosibirsk, 1974) [in Russian].
2. S. E. Haggerty, Nature **320**, 34 (1986).
3. H. O. A. Meyer, Mantle Xenoliths, Ed. by P. H. Nixon (Wiley, Chichester, 1987), p. 501.
4. E. M. Galimov, Geochim. Cosmochim. Acta **55** (6), 1697 (1991).
5. J. W. Harris, *The Properties of Natural and Synthetic Diamond,* Ed. by J. E. Field (Academic, London, 1992), p. 345.
6. G. P. Bulanova, J. Geochem. Explor. **53** (1–3), 1 (1995).
7. N. V. Sobolev and V. S. Shatsky, Nature **343**, 742 (1990).
8. O. Navon, *Proc. 7th Int. Kimberlite Conf. Red Roof Designs, Cape Town, 1999, p.* 584.
9. T. Stachel and J. W. Harris, Ore Geol. Rev. **34** (1–2), 5 (2008).
10. N. V. Sobolev, F. V. Kaminsky, W. L. Griffin, et al., Lithos **39**, 135 (1997).
11. N. V. Sobolev, A. M. Logvinova, D. A. Zedgenizov, et al., Lithos **77** (1–4), 225 (2004).
12. N. V. Sobolev, A. M. Logvinova, A. A. Tomilenko, et al., Geochim. Cosmochim. Acta **266**, 197 (2019).
13. N. P. Pokhilenko, N. V. Sobolev, V. N. Reutsky, et al., Lithos **77** (1–4), 57 (2004).
14. V. Shatsky, A. Ragozin, D. Zedgenizov, and S. Mityukhin, Lithos **105** (3–4), 289 (2008).
15. L. N. Kogarko and I. D. Ryabchikov, Petrology **21**, 316 (2013). https://doi.org/10.1134/S0869591113040048
16. S. B. Shirey, P. Cartigny, D. J. Frost, et al., Rev. Mineral. Geochem. **5** (1), 355 (2013).
17. F. V. Kaminsky, *The Earth's Lower Mantle: Composition and Structure* (Springer Geology, Switzerland, 2017).
18. F. V. Kaminsky, Earth-Sci. Rev. **110**, 127 (2012). https://doi.org/10.1016/j.earscirev.2011.10.005
19. V. K. Garanin, G. Yu. Kriulina, K. V. Garanin, et al., *Arkhangel'sk Diamonds: New Data* (IP Skorokhodov V.A., Moscow, 2018) [in Russian].
20. V. N. Kvasnitsa, *Small Diamonds* (Naukova Dumka, Kiev, 1985) [in Russian].
21. M. Schrauder and O. Navon, Geochim. Cosmochim. Acta **58** (2), 761 (1994).

22. E. S. Izraeli, J. W. Harris, and O. Navon, Earth Planet. Sci. Lett. **5807**, 1 (2001).
23. O. Klein-BenDavid, E. S. Izraeli, E. Hauri, et al., Lithos **77** (1–4), 243 (2004).
24. O. Klein-BenDavid, E. S. Izraeli, E. Hauri, et al., Geochim. Cosmochim. Acta **71**, 723 (2007). https://doi.org/10.1016/j.gca.2006.10.008
25. O. Klein-BenDavid, D. G. Pearson, G. M. Nowell, et al., Earth Planet. Sci. Lett. **289** (1–2), 123 (2010).
26. D. A. Zedgenizov, H. Kagi, V. S. Shatsky, et al., Mineral. Mag. **68** (1), 61 (2004).
27. A. A. Shiryaev, E. S. Izraeli, E. H. Hauri, et al., Russ. Geol. Geophys. **46**, 1185 (2005).
28. Y. Weiss, R. Kessel, W. L. Griffin, et al., Lithos **112**, 660 (2009).
29. A. A. Tomilenko, A. L. Ragozin, V. S. Shatskii, et al., Dokl. Akad. Nauk **378** (6), 802 (2001).
30. A. M. Logvinova, R. Wirth, A. A. Tomilenko, et al., Russ. Geol. Geophys. **52**, 1286 (2011).
31. S. Yu. Skuzovatov, D. A. Zedgenizov, A. L. Rakevich, et al., Russ. Geol. Geophys. **56**, 330 (2015). https://doi.org/10.1016/j.rgg.2015.01.024
32. N. V. Sobolev, E. M. Galimov, C. B. Smith, et al., Geol. Geofiz. **30**, 3 (1989).
33. T. Stachel, J. W. Harris, and G. P. Brey, Contrib. Mineral. Petrol. **132** (1), 34 (1998).
34. S. V. Titkov, A. I. Gorshkov, Yu. P. Solodova, et al., Dokl. Earth Sci. **410** (7), 1106 (2006).
35. E. M. Smith, S. B. Shirey, F. Nestola, et al., Science **354**, 1403 (2016). https://doi.org/10.1126/science.aal1303
36. V. S. Shatsky, A. L. Ragozin, A. M. Logvinova, et al., Lithos **364**, 105514 (2020). https://doi.org/10.1016/j.lithos.2020.105514
37. M. Schrauder and O. Navon, Nature **365** (6441), 42 (1993).
38. A. Wang, J. D. Pasteris, H. O. A. Meyer, et al., Earth Planet. Sci. Lett. **141**, 293 (1996).
39. V. Kvasnytsya, Diamond Relat. Mater. **39**, 89 (2013). https://doi.org/10.1016/j.diamond.2013.08.005
40. S. E. Haggerty, Geochem. Cosmochim. Acta **266**, 184 (2019). https://doi.org/10.1016/j.gca.2019.03.036
41. H. Bovenkerk, F. Bundy, H. Hall, et al., Nature **184**, 1094 (1959). https://doi.org/10.1038/1841094a0
42. A. A. Giardini and J. E. Tydings, Am. Mineral. **47**, 1393 (1962).
43. I. Sunagawa, in *Materials Science of the Earth's Interior,* Ed. by I. Sunagawa (Terra Scientific Publishing Company, Tokyo, 1984), p. 303.
44. A. S. Vishnevskii and O. V. Sukhodol'skaya, Mineral. Sb. Lviv Univ., No. 20 (4), 327 (1966).
45. H. M. Strong and R. M. Chrenko, J. Phys. Chem. **75**, 1838 (1971).
46. R. C. Burns, V. Cvetkovic, C. N. Dodge, et al., J. Cryst. Growth **104**, 257 (1990).
47. K. Sato and T. Katsura, J. Cryst. Growth **223**, 189 (2001). https://doi.org/10.1016/S0022-0248(01)00610-8
48. Yu. Pal'yanov, Yu. Borzdov, I. Kupriyanov, et al., Diamond Relat. Mater. **10**, 2145 (2001).
49. Y. N. Palyanov, I. N. Kupriyanov, Y. M. Borzdov, et al., Cryst. Growth Des. **9**, 2922 (2009). https://doi.org/10.1021/cg900265c
50. Yu. N. Palyanov, Yu. M. Borzdov, A. F. Khokhryakov, et al., Earth Planet. Sci. Lett. **250**, 269 (2006). https://doi.org/10.1016/j.epsl.2006.06.049
51. A. V. Shushkanova and Yu. A. Litvin, Can. Mineral. **46** (4), 991 (2008). https://doi.org/10.3749/canmin.46.4.991
52. Yu. N. Palyanov, Yu. M. Borzdov, A. F. Khokhryakov, et al., CrystEngComm (2020) (in press). https://doi.org/10.1039/d0ce00865f
53. Yu. N. Pal'yanov, A. G. Sokol, Yu. M. Borzdov, et al., Dokl. Akad. Nauk **363** (2), 230 (1998).
54. A. F. Khokhryakov, Yu. M. Borzdov, Yu. N. Pal'yanov, et al., Zap. Vseross. Mineral. O-va, No. 2, 105 (2003).
55. Y. N. Pal'yanov, A. G. Sokol, Y. M. Borzdov, et al., Nature **400**, 417 (1999).
56. Y. N. Pal'yanov, A. G. Sokol, Y. M. Borzdov, et al., Lithos **60**, 145 (2002).
57. Y. N. Palyanov, V. S. Shatsky, N. V. Sobolev, et al., Proc. Natl. Acad. Sci. U. S. A. **104**, 9122 (2007).
58. A. F. Shatskii, Yu. M. Bopzdov, A. G. Cokol, et al., Geol. Geofiz. **43** (10), 940 (2002).
59. Y. N. Palyanov and A. G. Sokol, Lithos **112S**, 690 (2009).
60. M. Arima, K. Nakayama, M. Akaishi, et al., Geology **21**, 968 (1993).
61. Yu. M. Borzdov, A. G. Sokol, Yu. N. Pal'yanov, et al., Dokl. Akad. Nauk **366** (4), 530 (1999).
62. Yu. N. Pal'yanov, V. C. Shatskii, A. G. Sokol, et al., Dokl. Earth Sci. **381**, 935 (2001).
63. Yu. N. Pal'yanov, A. G. Sokol, A. F. Khokhryakov, et al., Russ. Geol. Geophys. **56** (1–2), 196 (2015). https://doi.org/10.1016/j.rgg.2015.01.013
64. G. P. Brey, A. V. Girnis, V. K. Bulatov, et al., Contrib. Mineral. Petrol. **170**, 18 (2015). https://doi.org/10.1007/s00410-015-1166-z
65. Y. A. Litvin, *Genesis of Diamonds and Associated Phase* (Springer Mineralogy, 2017). https://doi.org/10.1007/978-3-319-54543-1
66. M. Akaishi, H. Kanda, and S. Yamaoka, Science **259**, 1592 (1993).
67. Yu. Pal'yanov, I. Kupriyanov, A. Khokhryakov, et al., Diamond Relat. Mater. **12**, 1510 (2003).
68. Y. N. Palyanov, I. N. Kupriyanov, A. G. Sokol, et al., Cryst. Growth Des. **11**, 2599 (2011). https://doi.org/10.1021/cg2003468
69. Y. N. Palyanov, Y. M. Borzdov, I. N. Kupriyanov, et al., CrystEngComm **17**, 4928 (2015). https://doi.org/10.1039/c5ce00897b
70. Y. N. Palyanov, I. N. Kupriyanov, A. F. Khokhryakov, et al., CrystEngComm. **19**, 4459 (2017).
71. S. Yamaoka, M. Akaishi, H. Kanda, et al., J. Cryst. Growth **125**, 375 (1992).
72. M. Akaishi, M. S. D. Kumar, H. Kanda, et al., Diamond Relat. Mater. **9**, 1945 (2000).

73. Yu. N. Pal'yanov, A. G. Sokol, A. F. Khokhryakov, et al., Dokl. Earth Sci. **375A**, 1395 (2000).
74. A. G. Sokol, Yu. N. Pal'yanov, G. A. Pal'yanova, et al., Diamond Relat. Mater. **10**, 2131 (2001).
75. A. G. Sokol and Y. N. Pal'yanov, Lithos **73** (1–2), S104 (2004).
76. A. J. Fagan and R. W. Luth, Contrib. Mineral. Petrol. **161**, 229 (2011). https://doi.org/10.1007/s00410-010-0528-9
77. Yu. N. Pal'yanov, A. G. Sokol, and N. V. Sobolev, Russ. Geol. Geophys. **46** (12), 1271 (2005).
78. H. Bureau, F. Langenhorst, A. L. Auzende, et al., Geochim. Cosmochim. Acta **77**, 202 (2012).
79. Y. N. Palyanov, Y. M. Borzdov, I. N. Kupriyanov, et al., Cryst. Growth Des. **12**, 5571 (2012). https://doi.org/10.1021/cg301111g
80. Y. N. Palyanov, A. F. Khokhryakov, Y. M. Borzdov, et al., Cryst. Growth Des. **13**, 5411 (2013). https://doi.org/10.1021/cg4013476
81. M. Moore and A. R. Lang, Philos. Mag. **26**, 1313 (1972).
82. B. Rondeau, E. Fritsch, and M. Moore, J. Cryst. Growth **304**, 287 (2007). https://doi.org/10.1016/j.jcrysgro.2007.03.004
83. Y. N. Pal'yanov, A. G. Sokol, Y. M. Borzdov, et al., Am. Mineral. **87**, 1009 (2002).
84. Y. N. Palyanov, I. N. Kupriyanov, A. G. Sokol, et al., Lithos **265**, 339 (2016). https://doi.org/10.1016/j.lithos.2016.05.021
85. Yu. N. Palyanov, Yu. M. Borzdov, A. F. Khokhryakov, et al., Cryst. Growth Des. **10**, 3169 (2010).
86. Yu. N. Pal'yanov, A. F. Khokhryakov, Yu. M. Borzdov, et al., Geol. Geofiz. **38** (5), 882 (1997).
87. A. A. Shiryaev, M. Wiedenbeck, and T. Hainschwang, J. Phys.: Cond. Matter **22**, 045801 (2010).
88. V. A. Nadolinny, O. P. Yuryeva, M. I. Rakhmanova, et al., Eur. J. Mineral. **24**, 645 (2012).
89. Y. Borzdov, Y. Pal'yanov, I. Kupriyanov, et al., Diamond Relat. Mater. **11**, 1863 (2002).
90. T. Evans, In *The Properties of Natural and Synthetic Diamond,* Ed. by J. E. Fields (Academic, London, 1992), p. 259.
91. R. M. Chrenko, R. E. Tuft, and H. M. Strong, Nature **270**, 141 (1977).
92. M. R. Brozel, T. Evans, and R. F. Stephenson, Proc. R. Soc. London, Ser. A **361**, 109 (1978).
93. B. P. Allen and T. Evans, Proc. R. Soc. London, Ser. A **375**, 93 (1981).
94. T. Evans, Z. Qi, and J. J. Maguire, Phys. C: Solid State Phys. **14**, L379 (1981).
95. T. Evans and Z. Qi, Proc. R. Soc. London, Ser. A **381**, 159 (1982).
96. Yu. A. Klyuev, A. M. Naletov, V. I. Nepsha, et al., Zh. Fiz. Khim. **56**, 524 (1982).
97. H. O. A. Meyer, H. J. Milledge, F. L. Sutherland, et al., Russ. Geol. Geophys. **38**, 305 (1997).
98. F. V. Kaminsky and G. K. Khachatryan, Can. Mineral. **39**, 1733 (2001).
99. K. De Corte, P. Cartigny, V. S. Shatsky, et al., Geochim. Cosmochim. Acta **62**, 3765 (1998). https://doi.org/10.1016/S0016-7037(98)00266-X
100. P. Cartigny, K. De Corte, V. S. Shatsky, et al., Chem. Geol. **176**, 265 (2001).
101. Y. Palyanov, I. Kupriyanov, A. Khokhryakov, et al., In *Handbook of Crystal Growth,* Ed. by P. Rudolph (Elsevier, Amsterdam, 2015), Vol. 2a, p. 671.
102. Z. Z. Liang, H. Jai, H. Kanda, et al., Carbon **44**, 913 (2006).
103. Y. Zhang, C. Zang, H. Ma, et al., Diamond Relat. Mater. **17**, 211 (2008).
104. Yu. N. Palyanov, Yu. V. Bataleva, A. G. Sokol, et al., Proc. Natl. Acad. Sci. U. S. A. **110**, 20408 (2013).
105. Yu. N. Pal'yanov and I. N. Kupriyanov, *Proc. II Int. Conf. "Crystallogenesis and Mineralogy," St. Petersburg, 2007,* p. 117.
106. I. N. Kupriyanov, Yu. N. Pal'yanov, A. G. Sokol, et al., *Proc. Int. Symp. "Petrology of Lithosphere and Origin of Diamond," Novosibirsk, June 5–7, 2008,* p. 48.
107. A. M. Zaitsev, V. S. Vavilov, and A. A. Gippius, Sov. Phys. Lebedev Inst. Rep. **10**, 15 (1981).
108. A. T. Collins, Diamond Relat. Mater. **1**, 457 (1992).
109. A. Tallaire, J. Achard, F. Silva, et al., Comp. Rend. Phys. **14**, 169 (2013).
110. G. Sittas, H. Kanda, I. Kiflawi, et al., Diamond Relat. Mater. **5**, 866 (1996).
111. A. M. Edmonds, M. E. Newton, P. M. Martineau, et al., Phys. Rev. B **77**, 245205 (2008).
112. U. F. S. D'Haenens-Johansson, A. M. Edmonds, B. L. Green, et al., Phys. Rev. B **84**, 245208 (2011).
113. C. M. Breeding and W. Wang, Diamond Relat. Mater. **17**, 1335 (2008).
114. M. Y. Lai, C. M. Breeding, T. Stachel, et al., Diamond Relat. Mater. **101**, 107642 (2020).
115. A. A. Shiryaev, A. V. Fisenko, I. I. Vlasov, et al., Geochim. Cosmochim. Acta **75**, 3155 (2011).
116. A. Komarovskikh, V. Nadolinny, Yu. Palyanov, et al., Phys. Status Solidi A **210**, 2074 (2013).
117. A. Komarovskikh, V. Nadolinny, Y. Palyanov, et al., Phys. Status Solidi A **211**, 2274 (2015).
118. T. Hainschwang, F. Notari, E. Fritsch, et al., Diamond Relat. Mater. **17**, 340 (2008).
119. G. Thiering and A. Gali, Phys. Rev. B **94**, 125202 (2016).
120. S. V. Titkov, R. M. Mineeva, N. N. Zudina, et al., Phys. Chem. Miner. **42**, 131 (2014).
121. A. E. Fersman, *Crystallography of Diamond* (Izd-vo AN SSSR, Moscow, 1955) [in Russian].
122. I. I. Shafranovskii, *Crystallography of Rounded Diamonds* (Izd-vo LGU, Leningrad, 1948) [in Russian].
123. A. A. Kukharenko, *Diamonds of the Urals* (Gosgeolizdat, Moscow, 1955) [in Russian].
124. Yu. L. Orlov, *Mineralogy of Diamond* (Nauka, Moscow, 1984) [in Russian].
125. Yu. L. Orlov, *Morphology of Diamond* (Izd-vo AN SSSR, Moscow, 1963) [in Russian].
126. M. Moore and A. R. Lang, J. Cryst. Growth **26**, 133 (1974).

127. D. N. Robinson, Miner. Sci. Eng. **10**, 55 (1978).
128. A. I. Chepurov, A. F. Khokhryakov, V. M. Sonin, et al., Dokl. Akad. Nauk SSSR, **285**, 212 (1985).
129. A. F. Khokhryakov and Yu. N. Pal'yanov, Mineral. Zh. **12** (1), 14 (1990).
130. A. F. Khokhryakov, Yu. N. Pal'yanov, and N. V. Sobolev, Dokl. Earth Sci. **381** (8), 884 (2001).
131. A. F. Khokhryakov, Yu. N. Pal'yanov, and N. V. Sobolev, Dokl. Earth Sci. **385** (8), 534 (2002).
132. Y. Kozai and M. Arima, Am. Mineral. **90**, 1759 (2005). https://doi.org/10.2138/am.2005.1862
133. A. F. Khokhryakov and Yu. N. Palyanov, Am. Mineral. **92**, 909 (2007). https://doi.org/10.2138/am.2007.2342
134. A. F. Khokhryakov and Yu. N. Palyanov, Am. Mineral. **95**, 1508 (2010). https://doi.org/10.2138/am.2010.3451
135. A. F. Khokhryakov and Y. N. Palyanov, Am. Mineral. **100**, 1528 (2015). https://doi.org/10.2138/am-2015-5131
136. Y. Fedortchouk, D. Canil, and E. Semenets, Am. Mineral. **92**, 1200 (2007). https://doi.org/10.2138/am.2007.2416
137. Y. Fedortchouk, Earth-Sci. Rev. **193**, 45 (2019). https://doi.org/10.1016/j.earscirev.2019.02.013
138. M. Arima and Y. Kozai, Eur. J. Mineral. **20**, 357 (2008). https://doi.org/10.1127/0935-1221/2008/0020-1820
139. A. G. Sokol, A. F. Khokhryakov, and Y. N. Palyanov, Contrib. Mineral. Petrol. **170**, 26 (2015). https://doi.org/10.1007/s00410-015-1182-z
140. D. Canil and A. J. Bellis, J. Petrol. **48**, 231 (2007). https://doi.org/10.1093/petrology/egl067
141. Z. V. Bartoshinskii and V. N. Kvasnitsa, *Crystal Morphology of Diamond from Kimberlites* (Naukova Dumka, Kiev, 1991) [in Russian].
142. V. P. Afanas'ev, E. S. Efimova, N. N. Zinchuk, and V. I. Koptil', *Atlas of the Morphology of Russian Diamonds* (Izd-vo NITs OIGGM SO RAN, Novosibirsk, 2000) [in Russian].
143. V. L. Skvortsova, A. A. Shiryaev, and Y. Fedortchouk, Diamond Relat. Mater. **104**, 107764 (2020). https://doi.org/10.1016/j.diamond.2020.107764
144. F. C. Frank, K. E. Puttic, and E. M. Wilks, Philos. Mag. **3**, 1262 (1958). https://doi.org/10.1080/14786435808233308
145. A. R. Lang, Proc. Roy. Soc. A **278**, 234 (1964).
146. S. Yamaoka, H. Kanda, and N. Setaka, J. Mater. Sci. **15**, 332 (1980).
147. A. F. Khokhryakov and Y. N. Palyanov, J. Cryst. Growth **502**, 1 (2018). https://doi.org/10.1016/j.jcrysgro.2018.09.008
148. A. F. Khokhryakov, D. V. Nechaev, and A. G. Sokol, Crystals **10**, 233 (2020). https://doi.org/10.3390/cryst10030233

Translated by Yu. Sin'kov